

Article

Templated Formation of Hydroxyapatite Nanoparticles from Self-Assembled Nanogels Containing Tricarboxylate Groups

Yoshihiro Sasaki^{1,2}, Setsuko Yamane³, Kei Kurosu¹, Shin-Ichi Sawada^{4,5}
and Kazunari Akiyoshi^{1,4,5,*}

¹ Institute of Biomaterials and Bioengineering, Tokyo Medical and Dental University, 2-3-10 Kanda-Surugadai, Chiyoda-ku, Tokyo 101-0062, Japan; E-Mails: yasaki.org@tmd.ac.jp (Y.S.); k.kurosu.bio@tmd.ac.jp (K.K.)

² PRESTO, Japan Science and Technology Agency, 4-1-8 Honcho Kawaguchi, Saitama 332-0012, Japan

³ Department of Chemistry and Biochemistry, Numazu National College of Technology, 3600 Ooka, Numazu 410-8501, Japan; E-Mail: syamane@numazu-ct.ac.jp

⁴ Graduate School of Engineering, Kyoto University, Katsura, Nishikyo-ku, Kyoto 615-8510, Japan; E-Mail: sawada@bio.polym.kyoto-u.ac.jp

⁵ ERATO, Japan Science and Technology Agency, 4-1-8 Honcho Kawaguchi, Saitama 332-0012, Japan

* Author to whom correspondence should be addressed; E-Mail: akiyoshi@bio.polym.kyoto-u.ac.jp; Tel.: +81-75-383-2589; Fax: +81-75-383-2590.

Received: 27 February 2012; in revised form: 10 April 2012 / Accepted: 11 April 2012 /

Published: 20 April 2012

Abstract: Nanosized hydroxyapatite (HAp) materials have received much attention in the context of their advanced biomedical applications, including tissue engineering and drug delivery systems. Hybridization of nanosized HAp with organic molecules is a promising approach to facilitate the preparation of HAp nanomaterials. Here, templated mineralization using self-assembled nanogels modified with tricarboxylate groups was performed to yield the hybrid HAp nanomaterial. In the pH gradient method, the nanogel acted as an excellent template for the formation of well-dispersed HAp particles. Transmission electron microscopy, selected area electron diffraction patterns and energy-dispersive X-ray spectroscopy of these particles revealed that amorphous nanoparticles of amorphous calcium phosphate formed first, followed by transformation to crystalline hydroxyapatite.

Keywords: nanogel; hydroxyapatite; organic-inorganic hybrid; calcium phosphate

1. Introduction

Hybrid organic-inorganic materials have many advantages because of their broad physical and chemical properties, which have led to innovative uses in diverse fields including optics, electronics, health care, energy and the environment [1–3]. One of the most important inorganic compounds is hydroxyapatite [HAp, $\text{Ca}_{10}(\text{PO}_4)_6(\text{OH})_2$], which is a major mineral component of natural bone and teeth. The similarity between HAp and these natural minerals has prompted extensive research to introduce HAp as a bone substitute or replacement [4,5].

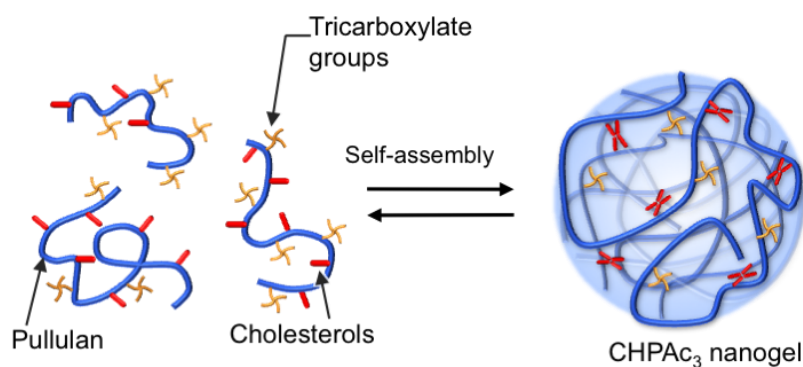
Nanosized HAp materials have also received much attention for advanced biomedical applications, including tissue engineering and drug delivery systems (DDS) [6]. Hybridization of HAp with organic molecules is a promising approach to develop functional HAp nanomaterials. There are several reports describing the preparation of hybrid HAp nanomaterials using surfactants [7], block copolymers [8] and liposomes [9] as organic components. Block copolymers with calcium phosphate nanoparticles showed enhanced cellular uptake. Hollow calcium phosphate nanospheres formed using surfactants and calcium phosphate-coated liposomes allowed controlled release of drugs. For further applications in advanced DDS, changes in the structural properties of hybrid HAp nanomaterials, including their size, colloidal stability, surface properties and crystallinity, will greatly affect their functions, including controlled release, cell-material interactions and biodegradability.

We previously reported that hydrogel nanoparticles (nanogels) of cholesterol-bearing pullulan (CHP) were used as a template for calcium phosphate mineralization to form well-dispersed hybrid nanoparticles (*ca.* 30 nm) in solution [10–12]. CHP nanogels are self-assembled physical gels in which hydrophobic cholesteryl groups provide physical cross-linking points [13]. One advantage of nanogels is that they can form a colloiddally stable complex with a protein with an overall complex size of about 50 nm, which is suitable for effective intracellular uptake. They also act as artificial chaperones to protect against the aggregation of denatured proteins and aid protein refolding [14]. These unique properties of nanogels are particularly valuable for cytokine delivery [15,16], cancer vaccines [17,18] and adjuvant-free intranasal vaccines [19]. However, the stability of CHP nanogels, especially in the bloodstream, is suboptimal because of their physical cross-linked structures. The formation of hybrid complexes of a nanogel with calcium phosphate may provide more stable DDS materials with controlled release properties. However, a limitation of calcium phosphate-CHP nanogel hybrid materials is that we only obtain amorphous or low-crystalline calcium phosphate as an inorganic component.

Amorphous calcium phosphate (ACP) readily dissolves in water. The crystallinity of calcium phosphate is an important factor for developing nanogel hybrid materials with adjustable controlled-release properties. The low crystallinity obtained using a CHP nanogel may be possible because of the lack of strong interactions between neutral CHP nanogels and calcium phosphate. Anionic functional moieties, such as carboxylate, sulfonate, silanol and phosphate, facilitate the mineralization of calcium phosphate [20–25]. Therefore, nanogels with functional groups will provide

a better template for the mineralization of calcium phosphate. In this study, we examined nanogel-templated mineralization using anionic nanogels, consisting of CHP, partially modified with tricarboxylate groups (CHPAC₃, Figure 1). These carboxylate CHP nanogels are expected to show increased affinity for calcium ions and thus induce the formation of calcium phosphate.

Figure 1. Schematic illustration showing nanogel formation of tricarboxylate-modified CHP (CHPAC₃). The CHPAC₃ forms monodisperse self-aggregates by intra- and/or intermolecular association in a diluted aqueous solution. The cholesterol groups provide noncovalent cross-linking points by aggregation, resulting in hydrogel nanoparticles with polycore structures.



2. Experimental Section

2.1. General

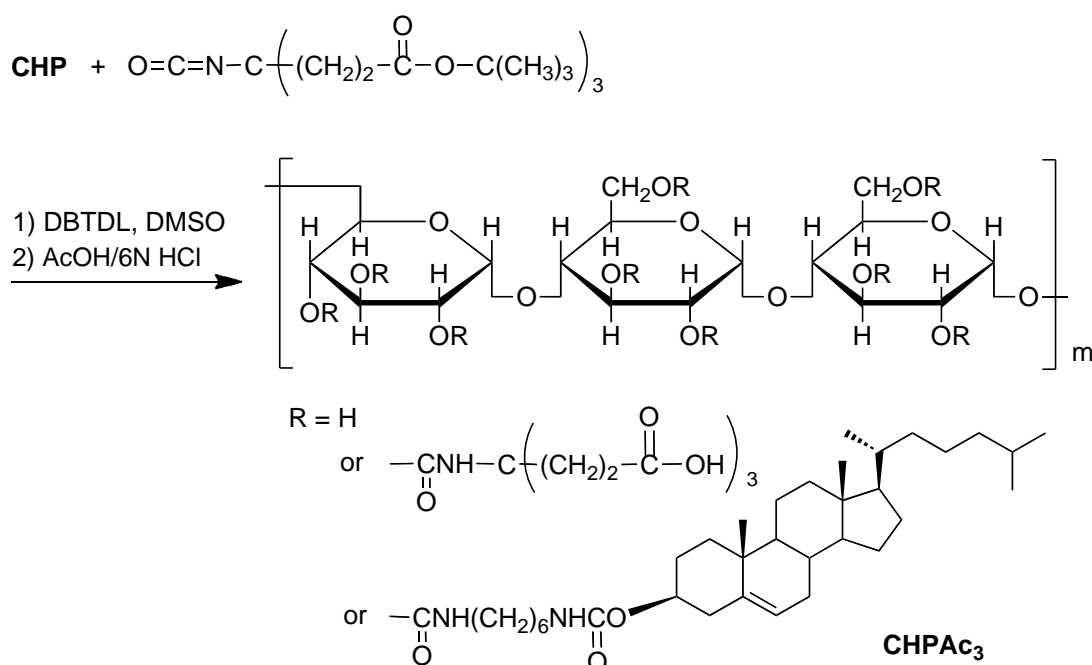
Organic solvents were purified, dried and kept over a drying agent before use. All reagents were commercially available with guaranteed grades, and were used without further purification. HAp was purchased from Taihei Chemical industrial Co., Ltd. (Osaka, Japan). CHP, which was substituted with 1.2 cholesteryl groups per 100 glucose units of the parent pullulan sample (mean molecular weight, 1.0×10^5 g/mol; Hayashibara Biochemical Laboratory, Inc., Okayama, Japan), was obtained as previously described [26]. The synthesis of CHPAC₃ is described below.

2.2. Synthesis of CHPAC₃

CHPAC₃ was synthesized by reacting the hydroxy groups of CHP with the isocyanate groups of Di-*t*-butyl-4-[2-(*t*-butoxycarbonyl)ethyl]-4-isocyanato-1,7-heptan dicarboxylate (Frontier Scientific, Inc, Utah, USA), followed by deprotection of the *t*-butoxycarbonyl (Boc) group, as shown in Figure 2. A solution of Di-*t*-butyl-4-[2-(*t*-butoxycarbonyl)ethyl]-4-isocyanato-1,7-heptan dicarboxylate (0.54 g) in anhydrous DMSO (10 mL) was added to a solution of CHP (1.14 g) in anhydrous DMSO (77 mL) containing dibutyltin dilaurate (0.23 mL). The solution was stirred at 45 °C for 24 h under a nitrogen atmosphere. The product was then precipitated with anhydrous EtOH/Et₂O (5:95) and washed with anhydrous EtOH/Et₂O (20:80). The precipitate was filtered and dried *in vacuo* to yield a white solid (0.50 g, 44%). Next, AcOH (3 mL) and 6 N aq. HCl (4 mL) were added dropwise to the Boc-protected CHPAC₃ (0.14 g)/DMSO (7 mL) solution. After stirring for 4 h, the product was precipitated with anhydrous EtOH/Et₂O (5:95). The precipitate was separated and purified by dialysis against Milli-Q

water using a seamless cellulose tube (molecular cut-off, 3,500 kDa), and finally lyophilized to yield a white powder (80.0 mg, 56%). $^1\text{H-NMR}$ (500 MHz, $\text{DMSO-}d_6/\text{D}_2\text{O}$ (9:1 v/v)), TMS): $\delta = 0.64$ (s, 3H; cholesterol 18- H_3), 0.70-2.40 (cholesterol H), 1.34 (27H; *t*-butyl), 1.77 (br, 6H; $\text{C}(\text{CH}_2\text{CH}_2\text{CO}_2\text{C}(\text{CH}_3)_3)_3$), 2.00 (br, 6H; $\text{C}(\text{CH}_2\text{CH}_2\text{CO}_2\text{C}(\text{CH}_3)_3)_3$), 4.7 (s, 33H per 100 glucose units, pullulan C^1H (1–6)), 5.0 (d, 66H per 100 glucose units, pullulan C^1H (1–4)). The number of tricarboxylate molecules coupled to the polysaccharides per 100 glucose units was 3.8, based on the integrated areas of the glucopyranosyl rings and tricarboxylate ethyl groups.

Figure 2. Synthesis of cholesterol- and tricarboxylate-bearing pullulan (CHPAc_3).



2.3. Preparation of the Nanogel Suspension

CHP or CHPAc_3 was suspended and swollen in Milli-Q water or buffer solution, and stirred for 12 h at 25 °C. The suspension was then sonicated using a probe-type sonicator (Sonifier 250, Branson Co., Ltd., Danbury, CT, USA; Tip diameter, 2 mm) at 40 W for 10 min under cooling with ice. The resulting suspension was filtered through 0.45- and 0.22- μm PVDF filters (Millex-HV, Millipore Co., Ltd., Billerica, MA, USA) to remove any impurities. This procedure yielded a clear aqueous solution.

2.4 Mineralization of Calcium Phosphate by the pH Gradient Method

Carbon dioxide gas was bubbled into a stirred suspension of HAp for 3 h at room temperature. The remaining solid HAp was then removed by filtration. The concentration of calcium ions in the solution was determined by back-titration using EDTA and Ca standard solution. The Ca^{2+} concentration was adjusted to 1.6 mM by adding water. The HAp solution (15 mL) was mixed with the nanogel suspension (15 mL) in a 100-mL pear-shaped flask ($[\text{Ca}^{2+}] = 0.8$ mM and 0.5 mg/mL nanogel) and stirred for 8 h at 25 °C. Calcium phosphate was precipitated by slowly increasing the pH of the solution from 5.6 to 7.9 over 8 h. The resulting solution was stored at 25 °C.

2.5. Characterization of the Nanomaterials

The hydrodynamic diameters and ζ -potentials were determined by photon correlation spectroscopy (PCS) analysis using a Zetasizer Nano ZS (Malvern Instruments, Malvern, UK). PCS was performed for triplicate samples at 25 °C. Sampling time and analysis were set to automatic. Particle size was determined as the z mean of three measurements. The measured autocorrelation function was analyzed by the cumulant method. The ζ -potential measurements were performed using a capillary ζ -potential cell in automatic mode. Transmission electron microscopy (TEM) images of unstained samples were taken with a Hitachi H-600 (Hitachi High-Technologies Co., Tokyo, Japan) at 100 kV. Energy-dispersive X-ray spectroscopy (EDS) measurements were obtained using a JEOL JEM-3010 equipped with an EDAX Genesis Series γ -TEM at 300 kV. Sample solutions were applied to a carbon-coated 100-mesh copper grid and excess samples were removed using filter paper.

3. Results and Discussion

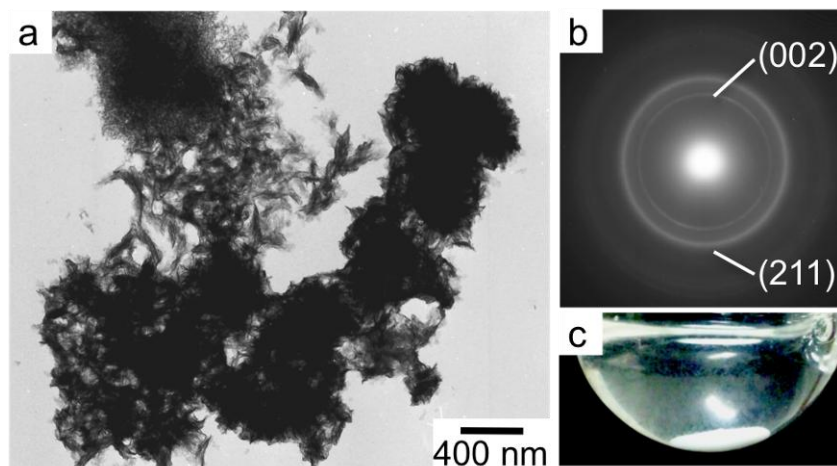
The hydrodynamic diameter of CHPAc₃ nanogels used in this study was 35 nm with a polydispersity index (PDI) of 0.23, as determined by dynamic light scattering. CHPAc₃ nanogels are slightly larger than conventional unmodified CHP, probably because of swelling of the nanogel embedded with highly anionic tricarboxylate groups. The ζ -potential of the CHPAc₃ nanogel was −13 mV compared with −2.3 mV for unmodified CHP nanogel, indicating that the highly anionic tricarboxylate groups were introduced, forming a negatively charged nanogel. Both nanogels were colloidally stable in solution for several months. Hybrids of the CHP or CHPAc₃ nanogels with calcium phosphate were then formed using the pH-gradient method [10]. Calcium phosphate was synthesized from a solution of HAp ($[\text{Ca}^{2+}] = 2.0 \text{ mM}$) by the pH gradient method, because calcium phosphate is more insoluble at basic pH. First, HAp was dissolved in acidic water by introducing CO₂ gas to the HAp solution. The nanogels were then added to this solution (0.5 mg mL^{-1}), which was subsequently stirred at 25 °C. The pH of the solution slowly increased from 5.6 to 7.9 with the loss of CO₂ gas.

TEM was performed to study the morphology of the mineralized samples. Since the samples were unstained, only inorganic materials are detected on the TEM images. We previously reported that CHP nanogels acted as effective templates for the formation of dispersed ACP nanoparticles at a low Ca²⁺ concentration (0.8 mM) [10]. We also found that the mineralization of calcium phosphate did not proceed at this dilute concentration of Ca²⁺ (0.8 mM) in the absence of CHP nanogels. On the other hand, large aggregated HAp crystals precipitated in the absence of CHP nanogels at a higher Ca²⁺ concentration (2.0 mM) [12]. These results suggest that ACP could be transformed to HAp crystals that are thermodynamically stable in this solution condition by increasing the Ca²⁺ concentration. To extend these findings, we examined the possibility of developing hybrid nanogel-HAp crystals using the pH gradient method under high Ca²⁺ concentrations with nanogels as a template or nuclei during mineralization.

In the presence of CHP nanogels, star-shaped inorganic nanoparticles, which were morphologically identical to typical HAp, were observed at higher Ca²⁺ concentrations (2.0 mM) (Figure 3a,b). However, the precipitation of aggregated HAp crystals, which is similar to that in the absence of CHP

nanogels [12], was observed on the TEM images, and the appearance of the solution (Figure 3c) suggested that the CHP nanogels were not effective for the preparation of well-dispersed hybrid nanoparticles.

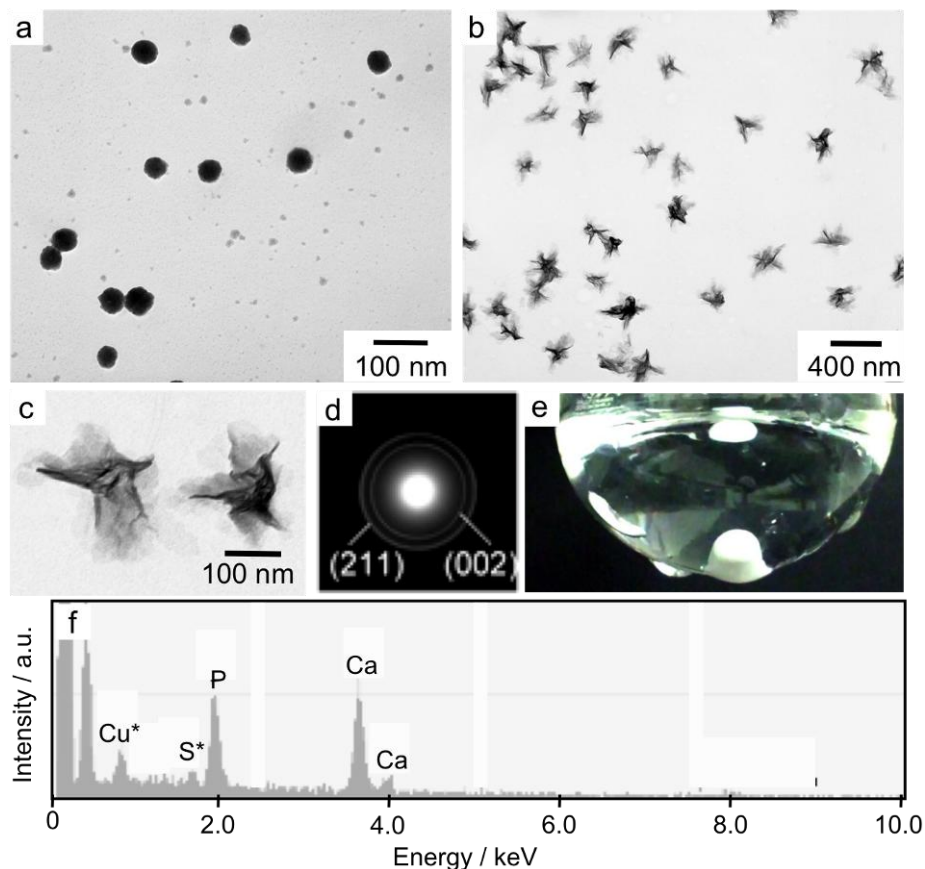
Figure 3. (a) TEM image of calcium phosphate nanoparticles formed in the presence of CHP nanogels (0.5 mg mL^{-1}) after 4 h of mineralization using the pH gradient method ($[\text{Ca}^{2+}] = 2.0 \text{ mM}$); (b) Analysis of the nanoparticles by selected area electron diffraction; (c) Appearance of the solution after mineralization.



Then, CHPAc_3 nanogels with tricarboxylate groups were investigated under the same conditions. Spherical inorganic nanoparticles corresponding to ACP with a mean diameter of 40 nm were observed in the early state of mineralization (1 h) (Figure 4a). After 4 h of incubation, well-dispersed inorganic nanoparticles, the hybrid nanogel-HAp nanoparticles, were formed in the presence of CHPAc_3 nanogels (Figure 4b,c). The suspension also looks transparent since the organic-inorganic nanoparticles were colloiddally well-dispersed without any precipitation to cause obvious light scattering (Figure 4e). The star-shaped nanoparticles were slightly larger than the particles shown in Figure 4a, indicating the accumulation of calcium phosphate onto the nanogel-ACP hybrid nanoparticles. Calcium phosphate could effectively nucleate in the CHPAc_3 nanogels because of the increase in the local concentration of Ca^{2+} by the interaction between the tricarboxylate groups and the dense polyhydroxy groups of the polysaccharide in the nanogel.

The mineralized nanoparticles obtained in the presence of CHPAc_3 nanogels were further analyzed by selected area electron diffraction (SAED) patterns and EDS. The distinct diffraction rings in the SAED patterns of the needle-shaped nanoparticles indicated that they were certainly crystal HAp (Figure 4d). The two most distinguishable rings correspond to the diffractions from the (002) and (211) planes of HAp, respectively. EDS showed that the Ca/P ratio in the hybrid nanoparticles was 1.5, which is similar to that of the original HAp (Figure 4f). The morphology and crystallinity of HAp were unchanged after 48 h for at least 4 months. The results indicate that the CHPAc_3 nanogels acted as excellent scaffolds for the nucleation of calcium phosphate as well as stabilization of calcium phosphate particles against aggregation to yield well-dispersed nanogel-HAp hybrids.

Figure 4. (a and b) TEM images of calcium phosphate nanoparticles formed in the presence of CHPAc₃ nanogels (0.5 mg mL⁻¹) after mineralization for 1 h (a) and 4 h (b) by the pH gradient method; (c) Magnified image of the star-shaped nanoparticles identified in (b); (d) Analysis of the nanoparticles by selected area electron diffraction; (e) Appearance of the aggregated solution; (f) SAED analysis of the area containing star-shaped nanoparticles.



4. Conclusions

Application of the pH gradient to self-assembled nanogels partially modified with tricarboxylate moieties and calcium phosphate yielded hybrid nanomaterials. These carboxylate nanogels acted as an effective template for the formation of well-dispersed nanosized calcium phosphate particles. The pH gradient method with relatively high concentrations of Ca²⁺ led to the formation of star-shaped HAp nanoparticles. These hybrid nanoparticles have a relatively narrow size distribution and are stable in solution for several months. Morphological observation of the formation of calcium phosphate in the presence of carboxylate nanogels revealed that ACP nanoparticles formed first, which was followed by transformation to crystalline HAp. The carboxylate nanogels efficiently prevented the aggregation of calcium phosphate nanoparticles during the phase-transition of ACP to HAp. These nanogel-calcium phosphate hybrid nanoparticles can be used as advanced drug and protein delivery systems, as well as for DNA transfection and bone regeneration, because of their biocompatibility and excellent biochemical characteristics.

Acknowledgments

This work was partially supported by a Grant-in-Aid for Scientific Research (A) (No. 20240047 to K.A. and Y.S.) and a Grant-in-Aid for Young Scientists (A) (No. 23681021 to Y.S.) from the Japan Society for the Promotion of Science (JSPS: “KAKENHI”). This work was also supported in part by a Grant-in-Aid for Scientific Research (No. 23107510) on the Innovative Areas: “Fusion Materials” (Area No. 2206) from the Ministry of Education, Culture, Sports, Science and Technology (MEXT).

References

1. Sanchez, C.; Belleville, P.; Popall, M.; Nicole, L. Applications of advanced hybrid organic-inorganic nanomaterials: From laboratory to market. *Chem. Soc. Rev.* **2011**, *40*, 696–753.
2. Vallet-Regi, M.; Colilla, M.; Gonzalez, B. Medical applications of organic-inorganic hybrid materials within the field of silica-based bioceramics. *Chem. Soc. Rev.* **2011**, *40*, 596–607.
3. Sasaki, Y.; Akiyoshi, K. Nanogel engineering for new nanobiomaterials: From chaperoning engineering to biomedical applications. *Chem. Rec.* **2010**, *10*, 366–376.
4. Hutmacher, D.W.; Schantz, J.T.; Lam, C.X.F.; Tan, K.C.; Lim, T.C. State of the art and future directions of scaffold based bone engineering from a biomaterials perspective. *J. Tissue Eng. Regen. Med.* **2007**, *1*, 245–260.
5. Habraken, W.; Wolke, J.G.C.; Jansen, J.A. Ceramic composites as matrices and scaffolds for drug delivery in tissue engineering. *Adv. Drug Deliv. Rev.* **2007**, *59*, 234–248.
6. Zhou, H.; Lee, J. Nanoscale hydroxyapatite particles for bone tissue engineering. *Acta Biomater.* **2011**, *7*, 2769–2781.
7. Tari, N.E.; Motlagh, M.K.M.; Sohrabi, B. Synthesis of hydroxyapatite particles in cationic mixed surfactants template. *Mater. Chem. Phys.* **2011**, *131*, 132–135.
8. Wagoner Johnson, A.J.; Herschler, B.A. A review of the mechanical behavior of CaP and CaP/polymer composites for applications in bone replacement and repair. *Acta Biomater.* **2011**, *7*, 16–30.
9. Chu, M.Q.; Liu, G.J. Preparation and characterization of hydroxyapatite/liposome core-shell nanocomposites. *Nanotechnology* **2005**, *16*, 1208–1212.
10. Sugawara, A.; Yamane, S.; Akiyoshi, K. Nanogel-templated mineralization: Polymer-calcium phosphate hybrid nanomaterials. *Macromol. Rapid Commun.* **2006**, *27*, 441–446.
11. Yamane, S.; Sugawara, A.; Sasaki, Y.; Akiyoshi, K. Nanogel-calcium phosphate hybrid nanoparticles with negative or positive charges for potential biomedical applications. *Bull. Chem. Soc. Jpn.* **2009**, *82*, 416–418.
12. Yamane, S.; Sugawara, A.; Watanabe, A.; Akiyoshi, K. Hybrid nanoapatite by polysaccharide nanogel-templated mineralization. *J. Bioact. Biocomp. Polym.* **2009**, *24*, 151–168.
13. Sasaki, Y.; Akiyoshi, K. Nanogel engineering for new nanobiomaterials: from chaperoning engineering to biomedical applications. *Chem. Rec.* **2010**, *10*, 366–376.
14. Sasaki, Y.; Akiyoshi, K. Development of an artificial chaperone system based on cyclodextrin. *Curr. Pharm. Biotechnol.* **2010**, *11*, 300–305.

15. Hasegawa, U.; Sawada, S.; Shimizu, T.; Kishida, T.; Otsuji, E.; Mazda, O.; Akiyoshi, K. Raspberry-like assembly of cross-linked nanogels for protein delivery. *J. Control Release* **2009**, *140*, 312–317.
16. Hirakura, T.; Yasugi, K.; Nemoto, T.; Sato, M.; Shimoboji, T.; Aso, Y.; Morimoto, N.; Akiyoshi, K. Hybrid hyaluronan hydrogel encapsulating nanogel as a protein nanocarrier: New system for sustained delivery of protein with a chaperone-like function. *J. Control Release* **2010**, *142*, 483–489.
17. Ikuta, Y.; Katayama, N.; Wang, L.; Okugawa, T.; Takahashi, Y.; Schmitt, M.; Gu, X.; Watanabe, M.; Akiyoshi, K.; Nakamura, H.; Kuribayashi, K.; Sunamoto, J.; Shiku, H. Presentation of a major histocompatibility complex class 1-binding peptide by monocyte-derived dendritic cells incorporating hydrophobized polysaccharide-truncated HER2 protein complex: implications for a polyvalent immuno-cell therapy. *Blood* **2002**, *99*, 3717–3724.
18. Kageyama, S.; Kitano, S.; Hirayama, M.; Nagata, Y.; Imai, H.; Shiraishi, T.; Akiyoshi, K.; Scott, A.M.; Murphy, R.; Hoffman, E.W.; Old, L.J.; Katayama, N.; Shiku, H.; Humoral immune responses in patients vaccinated with 1–146 HER2 protein complexed with cholesteryl pullulan nanogel. *Cancer Sci.* **2008**, *99*, 601–607.
19. Nochi, T.; Yuki, Y.; Takahashi, H.; Sawada, S.; Mejima, M.; Kohda, T.; Harada, N.; Kong, I.G.; Sato, A.; Kataoka, N.; Tokuhara, D.; Kurokawa, S.; Takahashi, Y.; Tsukada, H.; Kozaki, S.; Akiyoshi, K.; Kiyono, H. Nanogel antigenic protein-delivery system for adjuvant-free intranasal vaccine. *Nat. Mater.* **2010**, *9*, 572–578.
20. Boanini, E.; Fini, M.; Gazzano, M.; Bigi, A. Hydroxyapatite nanocrystals modified with acidic amino acids. *Eur. J. Inorg. Chem.* **2006**, *23*, 4821–4826.
21. Jiang, H.D.; Liu, X.Y.; Zhang, G.; Li, Y. Kinetics and template nucleation of self-assembled hydroxyapatite nanocrystallites by chondroitin sulfate. *J. Biol. Chem.* **2005**, *280*, 42061–42066.
22. Kawai, T.; Ohtsuki, C.; Kamitakahara, M.; Hosoya, K.; Tanihara, M.; Miyazaki, T.; Sakaguchi, Y.; Konagaya, S. In vitro apatite formation on polyamide containing carboxyl groups modified with silanol groups. *J. Mater. Sci. Mater. Med.* **2007**, *18*, 1037–1042.
23. Liu, Q.; Ding, J.; Mante, F.K.; Wunder, S.L.; Baran, G.R. The role of surface functional groups in calcium phosphate nucleation on titanium foil: A self-assembled monolayer technique. *Biomaterials* **2002**, *23*, 3103–3111.
24. Wong, A.T.C.; Czernuszka, J.T. Transformation behaviour of calcium phosphate 2. Effects of various phosphorylated amino acids. *Colloid Surf. A Physicochem. Eng. Asp.* **2005**, *103*, 23–36.
25. Granja, P.L.; Barbosa, M.A.; Pouysegu, L.; De Jeso, B.; Rouais, F.; Baquay, C. Cellulose phosphates as biomaterials. Mineralization of chemically modified regenerated cellulose hydrogels. *J. Mater. Sci.* **2001**, *36*, 2163–2172.
26. Akiyoshi, K.; Deguchi, S.; Moriguchi, N.; Yamaguchi, S.; Sunamoto, J. Self-aggregates of hydrophobized polysaccharides in water. Formation and characteristics of nanoparticles. *Macromolecules* **1993**, *26*, 3062–3068.